Monthly Notices
of the
ROYAL ASTRONOMICAL SOCIETY

MNRAS **487,** L86–L90 (2019)
Advance Access publication 2019 June 12

doi:10.1093/mnrasl/slz084

The mass density profile and star formation history of Gaussian and non-Gaussian clusters

R. R. de Carvalho,[1,2]★ A. P. Costa,[3] T. C. Moura[4] and A. L. B. Ribeiro[3]

[1]*NAT - Universidade Cruzeiro do Sul / Universidade Cidade de São Paulo, 01506-000, Brazil*
[2]*INPE / Divisão de Astrofísica, São José dos Campos 12227-010, Brazil*
[3]*Laboratório de Astrofísica Teórica e Observacional, Universidade Estadual de Santa Cruz - 45650-000, Ilhéus-BA, Brazil*
[4]*Dept. Astronomia, Instituto Astrofísico e Geofísico da USP, São Paulo 05508-090, SP, Brazil*

Accepted 2019 May 30. Received 2019 May 27; in original form 2019 April 4

ABSTRACT

This paper is the third of a series in which we investigate the discrimination between Gaussian (G) and Non-Gaussian (NG) clusters, based on the velocity distribution of the member galaxies. We study a sample of 177 groups from the Yang catalog in the redshift interval of $0.03 \leq z \leq 0.1$ and masses $\geq 10^{14}$ $M_{\odot}$. Examining the projected stellar mass density distributions of G and NG groups, we find strong evidence of a higher infall rate in the outskirts of NG groups over the G ones. There is a 61 per cent excess of faint galaxies in NGs when contrasted with G groups, when integrating from 0.8 to $2.0R/R_{200}$. The study of the star formation history (SFH) of ellipticals and spirals in the three main regions of the projected phase space reveals also that the star formation in faint spirals of NG groups is significantly different from their counterpart in the G groups. The assembled mass for faint spirals varies from 59 per cent at 12.7 Gyr to 75 per cent at 8.0 Gyr, while in G systems this variation is from 82 per cent to 91 per cent. This finding may also be interpreted as a higher infall rate of gas-rich systems in NG groups. This accretion process through the filaments, disturbing the velocity distribution and modifying not only the stellar population of the incoming galaxies but also their SFH, should be seriously considered in modelling galaxy evolution.

Key words: galaxies: clusters: general – galaxies:evolution – galaxies:formation – galaxies:star formation – galaxies:stellar content – galaxies: interactions.

1 INTRODUCTION

In the hierarchical structure formation framework (ΛCDM), clusters of galaxies grow from higher density regions in the large-scale structure of the early universe. In these regions, the galaxy formation process is likely to be accelerated, which explains qualitatively why the majority of star formation in galaxies located in the cluster central regions takes place much earlier ($z \gtrsim 1$) than that in the general field (e.g. van Dokkum et al. 1998, Kelson et al. 2000, Kodama & Bower 2003). The cluster formation is a continuous process and clusters may be found in different dynamical stages, as indicated by recent studies (Hou et al. 2009; Ribeiro et al. 2013; de Carvalho et al. 2017, Paper I; Roberts & Parker 2017; Costa, Ribeiro & de Carvalho 2018, Paper II). Hence, to understand the physical processes that drive galaxy evolution, it is imperative to analyse the properties of galaxies in different environments. Defining environment is no trivial task and it may be approached in different ways: local density, distance from cluster centre, halo mass, and, as more recently suggested, through the examination of the velocity distribution of galaxies in clusters, Gaussian (G) and non-Gaussian (NG) systems (de Carvalho et al. 2017). In the latter case, there is an important assumption made regarding the dynamics of the gravitational system – G systems are supposed to be in equilibrium (e.g. Ogorodnikov 1957; Lynden-Bell 1967).

An important parameter used to investigate the relation between galaxy properties and the environment in which they inhabit is the stellar mass, which provides an evolutionary trace of the galaxy population in terms of star formation rate and morphology (e.g. Bell et al. 2007, Cowie & Barger 2008, Foucaud et al. 2010), and it is also a possible discriminator of the distribution of the underlying dark matter in galaxy systems since stars are not expected to be stripped significantly because they are located deep in the galaxy potential and both, stars and dark matter, are collisionless (e.g. Andreon 2015; van der Burg et al. 2015). In this sense, Wang & Jing (2010) studying galaxy clustering in the Millennium Simulation, (Springel et al. 2005) proposed an empirical method to link galaxy stellar mass directly with its hosting dark matter halo mass. In that work, while the positions of galaxies are predicted by following the merging histories of haloes and the trajectories of sub-haloes in

★ E-mail: rrdecarvalho2008@gmail.com

the Millennium Simulation, the stellar mass of galaxies at $z \sim 0$ is related to the mass of the halo at the time when the galaxy was last the central dominant object.

All these studies relating the degree of Gaussianity of the velocity distribution to the properties of galaxies in groups/clusters (Ribeiro et al. 2013; de Carvalho et al. 2017; Costa et al. 2018) have proved the importance of assessing the velocity distribution, or even better the projected phase space (PPS), to gain more physical understanding of the processes operating in galaxies (Biviano et al. 2002; Muzzin et al. 2014; Jaffé et al. 2018). In this Letter, we focus our attention on the stellar mass distribution and the star formation history (SFH) of galaxies located in 177 groups selected by de Carvalho et al. (2017) from the Yang catalog (Yang et al. 2007). We describe the sample and methodology used in Section 2. The results obtained for the stellar mass distribution are presented in Section 3 followed by the analysis of the SFH in Section 4. Section 5 discusses the main findings of this contribution. We adopt a cosmology with $H_\circ = 72\,km\,s^{-1}\,Mpc^{-1}$, $\Omega_m = 0.3$, and $\Omega_\Lambda = 0.7$.

2 DATA AND METHODOLOGY

In this section, we briefly describe the sample, data, and the procedures used to identify the dynamical state of the groups. In the following analysis, we use 177 groups from the Yang group catalog representing systems with halo mass greater than $10^{14.0}\,M_\odot$, and classified as G or NG by de Carvalho et al. (2017). The Gaussianity of the velocity distribution of galaxies in clusters is measured using the so-called Hellinger Distance, a parameter that measures the distance between a given distribution and a G (see de Carvalho et al. 2017 for more details). The sample consists of 5068 galaxies in G groups and 2987 galaxies in NG's. We define the bright domain as ($0.03 \leq z \leq 0.1$ and $M_r \leq -20.55, \sim M^\star + 1$), where $M_r \leq -20.55$ is the limiting absolute magnitude, in r band, corresponding to the spectroscopic completeness of SDSS-DR7 at z = 0.1, while faint means ($0.03 \leq z \leq 0.04$ and $-20.55 < M_r \leq -18.44$). When we refer to the faint domain this includes only galaxies in groups in the redshift bin of $0.03 \leq z \leq 0.04$ probing the luminosity function down to $\sim M^\star + 3$. The parameters used in this investigation are presented in de Carvalho et al. (2017). Halo mass, M_{200}, and virial radius, R_{200}, were estimated using the shift-gapper analysis described in Lopes et al. (2009). Stellar masses were determined after characterizing the stellar population using the spectral fitting code STARLIGHT (Cid Fernandes et al. 2005). The stellar masses are determined within the fibre aperture and the extrapolation to the full extent of the galaxy is done by calculating the difference between fibre and model magnitudes in the z band (see de Carvalho et al. 2017).

As far as morphological classification, we have used the catalogue provided by the second edition of the Galaxy Zoo Project (hereafter Zoo2). This catalogue counts 243 500 bright, near, and large galaxies with available spectroscopic data in the seventh release of the SDSS data base. We have ∼80 per cent (4060/5068) of the galaxies in G Groups and ∼78 per cent (2344/2987) of the galaxies in NG Groups with morphological classes given by Zoo2. Finally, three different regions of the PPS are defined: Virial (VIR) – $0.0 < R/R_{200} < 0.5$ and $|\Delta V/\sigma| < 1.0$; backsplash (BS) – $1.0 < R/R_{200} < 1.5$ and $|\Delta V/\sigma| < 1.0$; and infall (INF) – $1.5 < R/R_{200} < 2.0$ and $1.0 < |\Delta V/\sigma| < 2.0$.

3 STELLAR MASS DISTRIBUTIONS

Although not much is known about the stellar mass distribution in clusters (e.g. Vulcani et al. 2013), recent works (e.g. Giodini et al. 2009; Annunziatella et al. 2014; van der Burg et al. 2014, 2015; Annunziatella et al. 2016) have been shedding some light into the properties of galaxies and their host environment by measuring the stellar mass density profiles Σ_M (the stellar mass included in each radial ring divided by its area). In this work, we use the stellar mass density profiles to investigate how galaxies are distributed in G and NG systems.

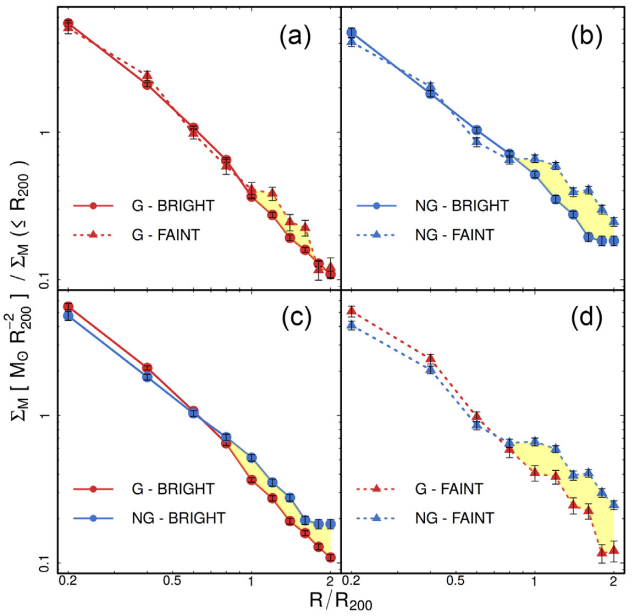

Figure 1. Projected surface stellar mass density profiles for the Yang clusters in our sample. In panel (a), we compare the bright and faint components of G groups, while in panel (b) we show how these two components behave in NG groups. Panel (c) exhibits the comparison between the bright component of Gs and NGs, and panel (d) compares the faint component of Gs and NGs. The error bars are displayed as the standard deviation, obtained by performing 1000 bootstraps of the stellar mass values in each radial ring. Notice that sometimes these error bars are smaller than the size of the symbols representing our estimates.

In Fig. 1, we show our stellar mass density profiles. Before we stack all systems belonging to each dynamic group, we normalize the projected radial distances by R_{200}, which ensures not to mix inner regions, virialized, with outer regions, non-virialized. The stellar mass densities were scaled by the stellar mass density corresponding to the virialized region ($\leq R_{200}$) for similar reasons to those considered in the normalization of the projected distances.

A common practice in this type of study is fitting the stellar mass density profiles with an NFW model (Navarro, Frenk & White 1997) to measure the total stellar mass of the system. However, this procedure brings an operational problem due to the fact that the stacked profile represents the mean distribution, disregarding the peculiarities of each system, and the amount of stellar mass, possibly significant, in-falling into the cluster. Since the NFW profile model does not consider the complexity of the data being fitted, in this work we choose, similar to Andreon (2015), not to perform this fitting. An example of the deviations of the NFW model from the surface mass density profiles can be found in Umetsu et al. (2014).

In Fig. 1, we show the stacked stellar mass density profile for the bright and faint components of the G and NG groups. In all panels, we see a clear excess of one component over the other (the yellow shaded area). We quantify this excess by doing numerical integration under the curves between two specific radius as indicated

below ($\int \Sigma_M/\Sigma_M(\leq R_{200})\,\mathrm{d}R$). We note that in stacking all the stellar mass density profiles of clusters in G and NGs, we normalize these stellar mass densities by the stellar mass density within the virialized region. This procedure implies losing the proper stellar mass density scale, which means that we are measuring only relative excesses.

In panel (a), we compare the faint and the bright components of G groups and we do observe a small excess of the faint over the bright (∼24 per cent) when we integrate from 1.0 to 2.0R/R_{200}. For NG systems (panel b), we see the same behaviour, although the excess of the faint over the bright component in the outer region (0.8 to 2.0R/R_{200}) is more pronounced (42 per cent). This might indicate a higher infall rate of low-mass galaxies in NG systems compared to Gs. From panel (c), we learn that the bright component in NG systems is also in clear excess (30 per cent) in the outskirts (from 0.8 to 2.0R/R_{200}) over the G groups. The same trend is present when comparing the faint components of Gs and NGs (panel d) – the faint component in NGs exhibits a considerable excess (61 per cent) in surface stellar mass density than their counterparts in Gs.

4 STAR FORMATION HISTORY

Our spectral analysis results not only in averaged age and metallicity but also in the SFH, which for a given galaxy is expressed by the contribution, as mass fraction, from each basis single stellar population. We estimate the cumulative fraction of stars older than a given age, as a function of the age of the basis. Therefore, the SFH is measured as the cumulative distributions over all galaxies in the sample within the two luminosity regimes, bright and faint. These luminosity regimes translate into two stellar mass domains, which here we list as the quartiles and median of the distributions ($Q_{25\ \mathrm{per\ cent}}$, Median, $Q_{75\ \mathrm{per\ cent}}$) – for the bright domain we have (10.30, 10.49, 10.65) and for the faint (9.26, 9.61, 9.89). Fig. 2 shows the SFH, expressed as the assembled mass versus the lookback time (LBT). The accuracy of the SFH is directly related to the age measurement. To assess how well we measure it, we use two different approaches: (1) Subsampling – where the resample size (70 per cent) is smaller than the sample size and resampling is done without replacement (1000 realizations); (2) Using repeated observations, which is dominated by bright galaxies. We use all galaxies in the sample with galaxy zoo classification, 4442 in the bright regime and 872 in the faint one. As for using the repeated observations, we have 2698 galaxies (6148 spectra). We quote the accuracy in SFH as $Q_\sigma = 0.7415$ ($Q_{75\ \mathrm{per\ cent}}$−$Q_{25\ \mathrm{per\ cent}}$). Using the repeated observations, we find that up to 3 Gyr the error is ∼1 per cent, from 3 to 8 Gyr is ∼6 per cent, reaching ∼14 per cent for ages larger than 10 Gyr. For faint galaxies (lower S/N), the errors are larger, up to 3 Gyr the error is ∼5 per cent, from 3 to 8 Gyr is ∼13 per cent, reaching ∼22 per cent for ages larger than 10 Gyr. Both methods of evaluating errors provide similar results.

In panel (a) of Fig. 2, bright galaxies in G systems, we see that ellipticals (in red) and spirals (in blue) have the same overall behaviour in assembling stellar mass *wrt* the environment. Galaxies in the VIR region (the solid line) tend to form stars earlier and faster than their counterpart in the general INF region (the dotted line). We also see that ellipticals and spirals, regardless of their position in the PPS, complete forming all their stars in the last 3 Gyr, except the spirals in the VIR and BS+INF regions of NG systems (panel d). Notice that at early stages (LBT∼ 13 Gyr) spirals have assembled only ∼75 per cent of their mass, while ellipticals already assembled at least ∼84 per cent, depending where they are located in the PPS. Ellipticals in the VIR region can accrete almost 95 per cent of their mass at LBT∼ 13 Gyr (monolithic scenario). Spirals, on the contrary, have a more gradual SFH, with those in the BS+INF region accreting 95 per cent of their mass only at LBT∼ 6 Gyr. This is the picture that emerges when focusing on the bright galaxies of G clusters, which is in agreement with results presented in Trevisan et al. (2012). We exhibit the SFH for faint galaxies in G systems in panel (b) of Fig. 2. The comparison with the bright galaxies reveals important aspects of the way galaxies evolve in relaxed systems. The faint ellipticals have their SFH very similar to the bright ones, although the ones in the INF region seem to have a more extended SFH (the dotted red line). Also, faint spirals have the same extended SFH, and again we see a more extended star formation for the ones in the BS+INF region. Notice also that ellipticals in the INF region look like spirals in the VIR+BS+INF regions. This may be partly reflecting our inability to properly classify galaxies when they are in the faint regime, namely spirals in VIR+BS+INF and ellipticals in the BS+INF represent systems that gradually form their stars until recently.

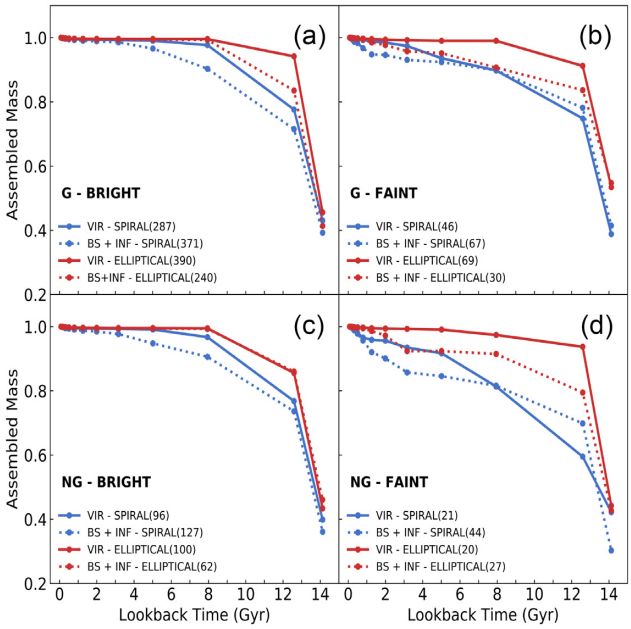

Figure 2. Fraction of assembled stellar mass as a function of the lookback time in Gyr, determined directly from the base ages. The solid red line represents ellipticals in the VIR region; The dotted red line means ellipticals in the BS+INF region. Symbols are the same for spirals but in blue. The Gaussianity as well as the luminosity regime probed is indicated in each panel. The number of galaxies in each morphological type and locus on the PPS are listed accordingly.

In panel (c) of Fig. 2, bright galaxies in NG systems, we note that ellipticals have the same SFH regardless of the environment, namely same behaviour in the VIR, BS, and INF regions, and similar to what we find for the bright galaxies in G systems. This result indicates that the dynamics of massive galaxies in NG systems is not significantly affected by the infall from the group surroundings. The same is true for the SFH for spirals, there seems to be no difference when comparing how star formation proceeds in spirals located in G or NG groups. In summary, we find that bright galaxies exhibit a similar SFH in G and NG systems, which reinforces previous findings for the age and metallicity distributions of these galaxies when comparing also G and NG groups (see de Carvalho et al. 2017). Finally, we examine the SFH of faint galaxies in NG groups and here the differences between G and NG are very significant.

Faint ellipticals in NG systems have their SFH similar to their counterparts in G systems. On the other hand, faint spirals in NG groups, display a very different behaviour in comparison with the G ones. In the BS+INF region, they accrete around 72 per cent of their mass at very early stages and then gradually form stars until recently (LBT$\sim$ 3 Gyr). They assemble $\sim$85 per cent of their mass and then experience a sudden growth of their stellar mass from $\sim$85 per cent to completion. In the VIR region, they have a steeper behaviour in SFH from early times up to 5 Gyr when then they evolve more slowly. These striking differences reinforce the differences between G and NG groups specially when we examine the faint galaxies in the outskirts (e.g. de Carvalho et al. 2017; Costa et al. 2018).

The overall picture that emerges from Fig. 2, when looking at the bright galaxies, is in agreement with previous works (e.g. Pérez-González et al. 2008, de La Rosa et al. 2011, Trevisan et al. 2012). Ellipticals in the VIR region, assemble more than 95 per cent of their mass at LBT $\sim$ 10 Gyr. Spirals in general form stars more gradually, exhausting the gas component only recently (Pérez-González et al. 2008). An important caveat in this analysis is that when we set a given galaxy to a specific position in the PPS, due to the statistical nature of this association, we introduce a certain variance in the SFH. The fraction of virialized, INF, and BS galaxies in cells of PPS, as listed by Mahajan, Mamon & Raychaudhury (2011), represents the probability of recovering a galaxy properly associated with the corresponding cells, namely VIR (89 per cent), BS (35 per cent), and INF (97 per cent).

5 DISCUSSION

Examining a sample of 319 groups from the Yang's catalog (Yang et al. 2007), de Carvalho et al. (2017) find that 76 per cent of the Yang's groups with masses above 10^{14} $M_{\odot}$ have G velocity distributions. Estimating skewness and kurtosis of the velocity distribution, they find evidence that faint galaxies in the outer regions of NG groups are infalling for the first time into the systems. Also, in the inner regions of G groups, galaxies are older and more metal-rich than their counterparts in NG systems. As far as the outer regions are concerned, galaxies of NG groups are older and more metal-rich than galaxies in G's, independent of their luminosity. These are clear indications of pre-processing in the outer parts of NG groups (Fujita 2004), in agreement with Roberts & Parker (2017). Costa et al. (2018) study the velocity dispersion profiles (VDPs) of G and NG systems and find that the stacked VDPs for G groups exhibit a central peak followed by a monotonically decreasing behaviour indicating predominantly radial orbits. The bright stacked VDPs show lower velocity dispersions than the faint stacked VDPs, in all radii. As far as NG systems, they display a distinct feature with a depression in the central region and also a likely higher infall rate associated with galaxies in the faint stacked VDP. These findings corroborate the Cava et al. (2017) results for regular and irregular systems. We note that what Cava et al. (2017) find for VDPs for regular systems are similar to that of a G system and the VDP for S galaxies in the irregular systems exhibit a depression in inner regions, similar to what Costa et al. (2018) find for the NG systems.

In this contribution, we investigate how the stellar mass distribution and the SFH of galaxies in clusters depend on the dynamical stage of groups/clusters. In de Carvalho et al. (2017), we present a robust technique to measure how the velocity distribution of galaxies is far from Gaussianity, and how that reflects the physical characterization of an out of equilibrium system. This distinction between G and NG systems is the base of our attempt to characterize the link between environment and galaxy properties.

We notice that, as pointed out by McGee et al. (2009) in their semi-analytic models, massive clusters ($>10^{14.5}$ $M_{\odot}$) at redshift zero have accreted 40 per cent of their galaxy members from the external environment. This gives further support to the idea presented here that it may be hard to find nearby clusters with perfect G velocity distribution and that Gaussianity, as measured in this paper, reflects the current infall rate. The projected surface stellar mass density profiles exhibit clear evidence of a higher infall rate between 1 and 2 R_{200} in NG groups compared to the G ones. The behaviour displayed in panels (a) and (b), with a clear excess of the faint component over the Bright one, is in agreement with results presented by Sánchez-Janssen, Aguerri & Muñoz-Tuñón (2008) who find an increase of the dwarf-to-giant ratio towards the outskirts of clusters. However, such an increase seems larger for NG systems considering that the excess of the faint component over the bright one for NG groups (42 per cent) is about twice as large as the excess measured for G systems (24 per cent). This result reinforces previous findings of de Carvalho et al. 2017; Costa et al. 2018), namely, a higher infall rate in NG groups disturbs the mean stellar population of galaxies and the velocity dispersion distribution of galaxies in the outskirts of these systems.

In recent years, a lot of attention has been paid to the question of what drives the evolution of galaxies in the outskirts of groups and clusters (Boselli et al. 2016; Jaffé et al. 2018). A galaxy in the vicinity of a rich cluster starts interacting gravitationally with other galaxies more frequently and also it senses the potential well of the system as a whole (Moore, Lake & Katz 1998). This may alter the stellar population properties of these infalling galaxies. Therefore, we do expect significant variations of their SFH specially when we probe the PPS for different morphological types. In this work, we find that bright ellipticals in the VIR region (panels a and c of Fig. 2), assemble more than 95 per cent of their mass at LBT $\sim$ 10 Gyr, regardless if they are in G or NG systems, which is a somewhat expected result (Trevisan et al. 2012). Bright spirals assemble their stellar mass in a similar way comparing G and NG groups, independent of the PPS region. As far as faint galaxies go, we see a very different behaviour. Faint ellipticals have similar SFH in G and NG groups and they are equally old in both systems (de Carvalho et al. 2017; Einasto et al. 2018). However, the SFH of faint spirals in NG systems is considerably dissimilar to those in G groups. The SFH of faint spirals in the VIR region of NG groups grows more slowly than their counterpart in G groups. This can be interpreted as further evidence of a higher infall rate in NG systems.

In summary: bright galaxies (ellipticals and spirals) seem to have similar SFH independent of where they are located in the PPS, faint ellipticals also have similar SFH regardless the location in the PPS, and the key difference arises when we examine faint spirals in the VIR and BS+INF regions – SFH of galaxies in the VIR region belonging to NG groups is far more gradual. These conclusions are critically important considering that if the distinction between G and NG is not made, this can imply a potentially serious problem in modelling galaxy evolution in clusters.

ACKNOWLEDGEMENTS

RRdC thanks Francesco La Barbera, Gary Mamon, Joseph Silk and Tatiana Laganá for fruitful discussions on this subject. APC thanks Coordenação de Aperfeiçoamento de Pessoal de Nível Superior for financial support. ALBR thanks Conselho Nacional de Pesquisa e Desenvolvimento, grant 311932/2017-7. RRdC and TCM acknowledge financial support from Fundacão de Amparo a

Pesquisa do Estado de São Paulo through grants 2014/11156-4 and 2018/03480-7, respectively.

REFERENCES

Andreon S., 2015, A&A, 575, A108
Annunziatella M. et al., 2014, A&A, 571, A80
Annunziatella M. et al., 2016, A&A, 585, A160
Bell E. F., Zheng X. Z., Papovich C., Borch A., Wolf C., Meisenheimer K., 2007, ApJ, 663, 834
Biviano A., Katgert P., Thomas T., Adami C., 2002, A&A, 387, 8
Boselli A. et al., 2016, A&A, 596, A11
Cava A. et al., 2017, A&A, 606, A108
Cid Fernandes R., Mateus A., Sodré L., Stasińska G., Gomes J. M., 2005, MNRAS, 358, 363
Costa A. P., Ribeiro A. L. B., de Carvalho R. R., 2018, MNRAS, 473, L31
Cowie L. L., Barger A. J., 2008, ApJ, 686, 72
de La Rosa I. G., La Barbera F., Ferreras I., de Carvalho R. R., 2011, MNRAS, 418, L74
de Carvalho R. R., Ribeiro A. L. B., Stalder D. H., Rosa R. R., Costa A. P., Moura T. C., 2017, AJ, 154, 96
Einasto M. et al., 2018, A&A, 610, A82
Foucaud S., Conselice C. J., Hartley W. G., Lane K. P., Bamford S. P., Almaini O., Bundy K., 2010, MNRAS, 406, 147
Fujita Y., 2004, PASJ, 56, 29
Giodini S. et al., 2009, ApJ, 703, 982
Hou A., Parker L. C., Harris W. E., Wilman D. J., 2009, ApJ, 702, 1199
Jaffé Y. L. et al., 2018, MNRAS, 476, 4753
Kelson D. D., Illingworth G. D., van Dokkum P. G., Franx M., 2000, ApJ, 531, 184
Kodama T., Bower R., 2003, MNRAS, 346, 1
Lopes P. A. A., de Carvalho R. R., Kohl-Moreira J. L., Jones C., 2009, MNRAS, 399, 2201
Lynden-Bell D., 1967, MNRAS, 136, 101
Mahajan S., Mamon G. A., Raychaudhury S., 2011, MNRAS, 416, 2882
McGee S. L., Balogh M. L., Bower R. G., Font A. S., McCarthy I. G., 2009, MNRAS, 400, 937
Moore B., Lake G., Katz N., 1998, ApJ, 495, 139
Muzzin A. et al., 2014, ApJ, 796, 65
Navarro J. F., Frenk C. S., White S. D. M., 1997, ApJ, 490, 493
Ogorodnikov K. F., 1957, Sov. Astron., 1, 748
Pérez-González P. G. et al., 2008, ApJ, 675, 234
Ribeiro A. L. B., de Carvalho R. R., Trevisan M., Capelato H. V., La Barbera F., Lopes P. A. A., Schilling A. C., 2013, MNRAS, 434, 784
Roberts I. D., Parker L. C., 2017, MNRAS, 467, 3268
Sánchez-Janssen R., Aguerri J. A. L., Muñoz-Tuñón C., 2008, ApJ, 679, L77
Springel V. et al., 2005, Nature, 435, 629
Trevisan M., Ferreras I., de La Rosa I. G., La Barbera F., de Carvalho R. R., 2012, ApJ, 752, L27
Umetsu K. et al., 2014, ApJ, 795, 163
van der Burg R. F. J., Muzzin A., Hoekstra H., Wilson G., Lidman C., Yee H. K. C., 2014, A&A, 561, A79
van der Burg R. F. J., Hoekstra H., Muzzin A., Sifón C., Balogh M. L., McGee S. L., 2015, A&A, 577, A19
van Dokkum P. G., Franx M., Kelson D. D., Illingworth G. D., 1998, ApJ, 504, L17
Vulcani B. et al., 2013, A&A, 550, A58
Wang L., Jing Y. P., 2010, MNRAS, 402, 1796
Yang X., Mo H. J., van den Bosch F. C., Pasquali A., Li C., Barden M., 2007, ApJ, 671, 153

This paper has been typeset from a TEX/LATEX file prepared by the author.